PROTEINS
STRUCTURE ■ FUNCTION ■ BIOINFORMATICS

SHORT COMMUNICATION

Molecular simulations enlighten the binding mode of quercetin to lipoxygenase-3

Sébastien Fiorucci, Jérôme Golebiowski, Daniel Cabrol-Bass, and Serge Antonczak*

Laboratoire de Chimie des Molécules Bioactives et des Arômes, UMR-CNRS 6001, Faculté des Sciences, Université de Nice Sophia Antipolis, 06108 Nice Cedex 2, France

ABSTRACT

Inhibition of lipoxygenases (LOXs) by flavonoid compounds is now well documented, but the description of the associated mechanism remains controversial due to a lack of information at the molecular level. For instance, X-ray determination of quercetin/LOX-3 system has led to a structure where the enzyme was cocrystallized with a degradation product of the substrate, which rendered the interpretation of the reported interactions between this flavonoid compound and the enzyme difficult. Molecular modeling simulations can in principle allow obtaining precious insights that could fill this lack of structural information. Thus, in this study, we have investigated various binding modes of quercetin to LOX-3 enzyme in order to understand the first step of the inhibition process, that is the association of the two entities. Molecular dynamics simulations and free energy calculations suggest that quercetin binds the metal center via its 3-hydroxychromone function. Moreover, enzyme/substrate interactions within the cavity impose steric hindrances to quercetin that may activate a direct dioxygen addition on the substrate.

Proteins 2008; 73:290–298.

Key words: flavonoid; dioxygenase; inhibition; enzyme/substrate interactions; binding free energy; molecular dynamics.

INTRODUCTION

Lipoxygenases (LOXs) constitute a family of peroxidizing enzymes that catalyze regioselective and stereospecific dioxygenation of polyunsaturated fatty acid (PUFA), yielding hydroperoxide derivatives known, for example, as precursors of inflammatory mediators, as leukotrienes or lipoxins in the mammals.[1–3] Because of the implication of LOXs in various pro-oxidant biological processes, research of effective inhibitors is still of much interest. The number of articles treating of this subject has deeply increased these past 4 years and some recent reviews[4–6] give a good overview concerning LOX inhibition. Catechol derivatives like nordihydroguaiaretic acid (NDGA), 4-nitrocatechol, caffeic acid, or flavonoids have been identified as inhibiting LOXs[7–9] but molecular descriptions related to these processes have not yet been clearly established. Competitive reversible and irreversible inhibition schemes, as well as inhibition via reduction of the enzyme-bound radical intermediate have been considered to explain the activity of polyphenolic compounds. Moreover, heterogeneity in the interpretation of the experimental results of the inhibition processes, for example concerning kinetic data, prevents converging toward a general way of inhibition. Flavonoids, polyphenol derivatives present in substantial amounts in plants, are able to interfere in biological processes involving reactive oxygen species (ROS). Indeed, they have strong antioxidative and free radical scavenging properties[10,11] due to their highly functionalized rings. Thus, quercetin, one of the most predominant flavonol in plants, is reported to inhibit 5-LOX, 12-LOX, 15-LOX, and LOX-1 with a significant IC_{50} value.[4,12,13]

Among plant LOXs, soybean lipoxygenase isozyme 1 (LOX-1) can be regarded as the mechanistic paradigm for these nonheme iron dioxyge-

Additional Supporting Information may be found in the online version of this article.

Sebastien Fiorucci's current address is School of Engineering and Science, Jacobs University Bremen, Campus Ring 1, D-28759 Bremen, Germany.
*Correspondence to: Serge Antonczak, Laboratoire de Chimie des Molécules Bioactives et des Arômes, UMR-CNRS 6001, Faculté des Sciences, Université de Nice Sophia Antipolis, 06108 Nice Cedex 2, France.
E-mail: Serge.Antonczak@unice.fr
Received 15 February 2008; Revised 6 June 2008; Accepted 9 June 2008
Published online 24 July 2008 in Wiley InterScience (www.interscience.wiley.com).
DOI: 10.1002/prot.22179

nase.[2,14,15] Indeed, cofactor cycles between the catalytically active (ferric) Fe(III) state and the inactive (ferrous) Fe(II) one have been reported.[16,17] In this mechanistic scheme, the first step of the PUFA degradation by LOX is assumed to be a hydrogen transfer between the substrate and the metal center via a hydroxide ion coordinated to the iron ion (Fe(III)—OH → Fe(II)—OH_2). Then, after dioxygen addition on the radical intermediate, the peroxide binds the metal center in a so-called iron-peroxide complex, identified as a "purple" LOX.[18–20]

Lipoxygenase-3 (LOX-3) X-ray structure has also been reported, but this isozyme possesses some differences concerning its catalytic cycle with respect to LOX-1 although they share similar sequence and folding.[21] However, structurally speaking, it has been reported that not only the size and shape of the internal cavities adjoining the metal center but also the substitution of some specific residues affect the stereospecificity and regioselectivity of the FA degradation[3] as well as the inhibition process.[22,23] Surprisingly, a structural analysis of LOX-3 crystals soaked with quercetin has recently revealed the enzyme in complex with a degradation product of the flavonoid positioned near the active site (PDB ID: 1N8Q).[24] This result was unexpected because quercetin was described as a competitive inhibitor. However, such processes have already been reported with other polyphenol inhibitors such as curcumin and epigallocatechin gallate (EGCG).[25,26] As mentioned in a recent review,[4] the following question arises: "What is really inhibiting LOX, a given chemical or its LOX metabolite?". Indeed, in an aqueous environment, quercetin can be easily oxidized in the presence of iron and free radicals.[27–30] X-ray radiations are able to generate such free radicals leading to the formation of a highly reactive species of the flavonoid (semiquinone) facilitating the cooxidation process and, at the end, the inhibition of LOX by the reaction product, namely. the protocatechuic acid when quercetin is considered. This multistep mechanism could enlighten why the inhibition process is so complex on a kinetic point of view.[4] In conclusion, authors suggest a degradation of the flavonoid triggered by X-ray and catalyzed by the protein.[24–26]

Without compromising this multistep process, chelation to the active site followed by degradation of the flavonoid by dioxygen addition should, however, not be excluded. In this case, an opening of the C-ring is necessary to generate the protocatechuic acid. Such a mechanism has already been described considering Quercetin 2,3-Dioxygenase (Q23D),[31] an other dioxygenase. In this mechanism, quercetin is deprotonated by a glutamate amino acid located in the active site and oxidized by the metal center. The formation of the semiquinone species is required otherwise the addition of dioxygen onto the flavonoid would be a spin-forbidden process. Then, as a result of the mechanism, carbon monoxide and the degradation product are released. According to the structural determination mentioned earlier one could imagine that such degradation is likely to occur in LOX-3 enzyme. A hydrolysis of the benzoic acid ester should then take place and lead to the production of the protocatechuic acid.

Following this hypothesis, the way quercetin binds the metal center still need to be addressed. Several modes of interaction and activation may be envisaged because quercetin has five hydroxyl groups that can be deprotonated and linked to the metal center and thus be at the origin of the degradation process. Concerning deprotonation of the flavonoid, it can be considered that Ile857 plays the role of proton acceptor. Structurally speaking, according to the protocatechuic acid/LOX-3 X-ray structure, both Ile857 oxygen atom and inhibitor O4′ atom show a clear proximity (2.7 Å). However, the position of this small molecule in the cavity should be considered with care because protocatechuic acid is small enough to reorganize within the enzyme cavity.[23] Thus, quercetin deprotonation could involve other hydroxyl sites. Therefore various binding mode have been considered in this work. Indeed, in addition to a catechol moiety, quercetin has different functional groups able to bind a metal (see Fig. 1). If a degradation mechanism similar to the one occurring in quercetinase is anticipated, the 3-hydroxychromone binding site should coordinate the active site. Another binding mode can be considered because the 7-OH function of the degradation product of EGCG was found at a distance of 2.7 Å to the metal center in the X-ray structure (PDB ID: 1JNQ). The possibility that the 5-hydroxychromone site binds the iron cation has been excluded because strong steric hindrances between the flavonoid and residues constituting the active site are generated. Moreover, on the basis of previous work, such activation of the C-ring is not effective[32] for dioxygen addition. As a summary, in this study, we report theoretical investigations concerning three binding modes between quercetin and LOX-3 enzyme. Thus O3, O7, and O4′ oxygen atoms have been considered to bind the iron center. These specific interactions lead then, through electron transfer from the substrate to the cation, to semiquinone forms, and related tautomeric structures, that are compatible with an addition of the triplet spin state dioxygen to the flavonol squeleton.

METHODOLOGY

Quercetin: C-terminal residue and iron parameters

On the basis of hypotheses raised earlier, quercetin is coordinated to the metal center and is assumed to be activated by both hydrogen and electron transfers. Thus, iron is in a +II oxidation state, the C-terminal residue is protonated, and quercetin is deprotonated and oxidized. Therefore, three semiquinone forms[32] for quercetin have

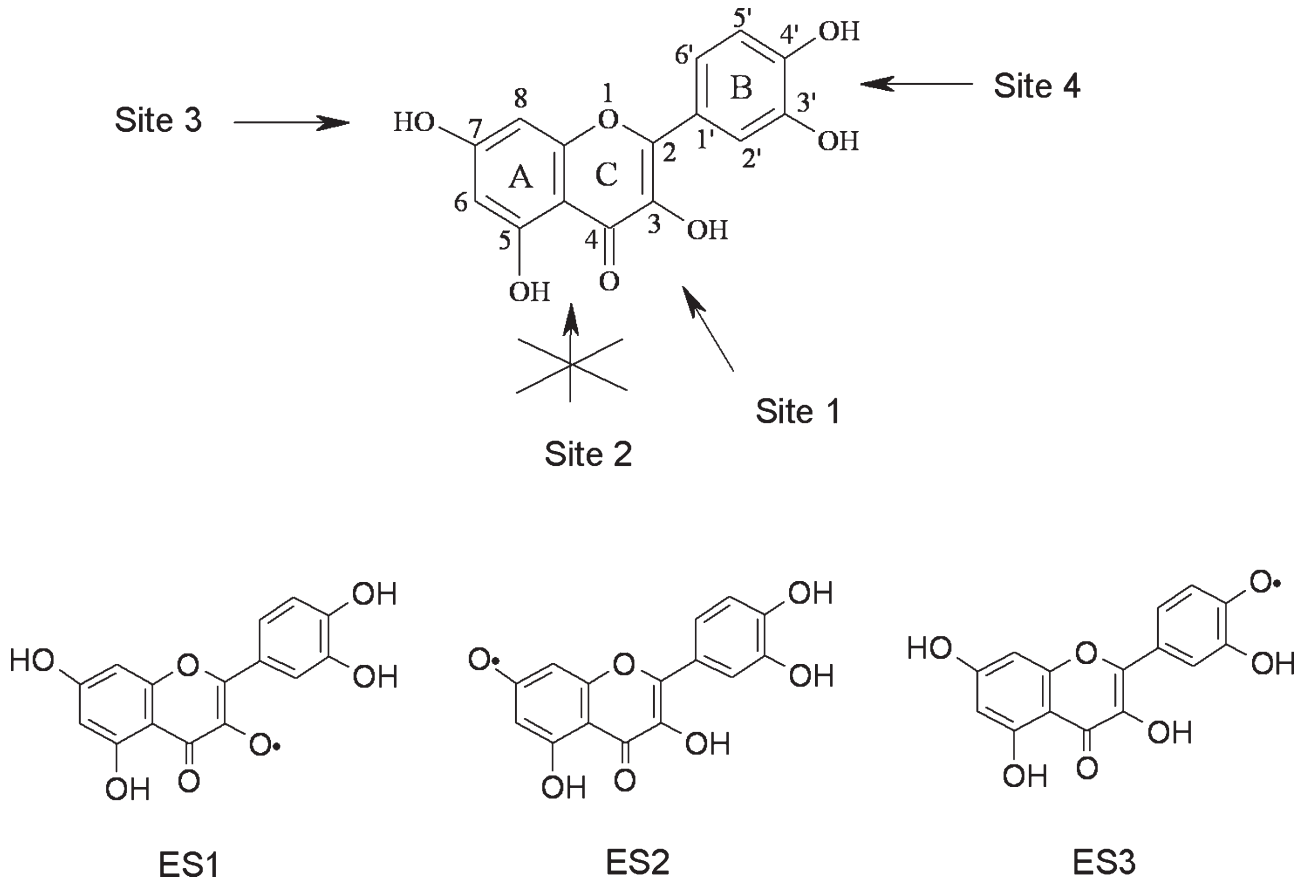

Figure 1

Quercetin semiquinone forms considered in this study: in O3, O7 and O4′ associated to ES1, ES2 and ES3 simulations respectively. The possible chelation sites to the metal are also shown.

been considered, at the O3, O7, and O4′ positions (see Fig. 1). Concerning these activated forms, bond angle and torsion-angle parameters have been assigned on the basis of structures optimized at the B3LYP[33–35]/6-31(+)G*[36–39] level of theory, using GAUSSIAN03[40] program. Such a level of computation has previously been shown to reproduce fairly well the structural parameters of similar systems.[41] Atomic charges for the three deprotonated oxidized quercetin have been obtained following the RESP charge fitting procedure using B3LYP/6-31(+)G* electrostatic potential. Detailed parameters can be found in Supplementary Material section. The metal center has been considered as a cation, and no bond restraint was applied between the iron and the ligands. Fe(II) parameters can be resumed as: $q = +2$, $r_{vdw} = 1.200$, $\varepsilon_{vdw} = 0.050$. To obtain partial atomic charges of the neutral C-terminal residue (ILE857), we have followed the standard antechamber[42] procedure implemented in the AMBER8[43] program on an ACE-ILE compound. ACE corresponds to an acetyl functional group and fills the valence of the N atom of the ILE residue. CM2 charges,[44] atom types[45] as well as bond angle and torsion angle can be found in supplementary material.

Definition of the system

The three initial structures for LOX-3/quercetin complexes have been manually built using EGC/LOX-3 structure (PDB ID: 1JNQ). This structure provides a bigger internal cavity,[23] which makes easier the insertion of quercetin semiquinone forms following the three hypotheses mentioned above. Note also that the volumes occupied by EGC and quercetin are similar. Moreover, it appeared that it was not mandatory to obtain suggestions from docking calculations because the three initial positions of quercetin semiquinone forms had to account for indications given by the putative degradation mechanisms and the possible stabilizations and destabilizations by the amino acids of the inner surface of the enzyme cavity. Simulations of the LOX-3/quercetin complexes will be noted ES1, ES2, and ES3 for the binding modes involving the 3-OH, 7-OH, and 4′-OH hydroxyl groups,

respectively. Concerning ES1 complex, quercetin was positioned in the cavity following indications given by the docking study carried out by Borbulevych *et al.*[23,24] In the ligand, O3 atom is in the first coordination sphere of the metal center, and O5 is located close to the C-terminal residue. Concerning ES2 complex, quercetin was placed to fit the most adequately EGC position. Concerning the ES3 complex, we have positioned quercetin so that B-ring is superimposed with C-ring from the ES2 structure. Five hundred and eleven water molecules initially present in X-ray structure have been kept for all the three complexes. The systems have been neutralized by addition of 10 Na^+ counter-ions placed in the most negative regions of space using the LEAP module. The water phase was then extended to a distance of 9.5 Å from any solute atom. Each system has been embedded in a periodic box containing 27763 (ES1 and ES2) and 27764 (ES3) TIP3P water molecules.

Molecular dynamics

Simulations were performed using the AMBER8 program and GAFF and parm99 forcefields parameters. Molecular dynamics simulations were carried out in the isothermal–isobaric ensemble at 310 K with the SANDER module using SHAKE on bonds involving hydrogen atoms. A time step of 2 fs was applied. A 8 Å cutoff was applied to nonbonded van der Waals interactions and the nonbonded pair list was updated every 25 steps. Once the ions and the water molecules were added to the initial structure, 2000 steps of minimization keeping the solute and the ions fixed, followed by 2000 steps of minimization keeping the solvent fixed were performed using particle mesh Ewald (PME) summation method. The equilibration runs continued by an equilibration of 50 ps of PME dynamics, keeping the solute fixed. Then, 2000 steps of minimization and 50 ps of MD simulation using a restraint of 30 kcal mol^{-1} $Å^{-2}$ on the solute atoms were performed followed by six rounds of 2000 steps minimization reducing the restraints by 5 kcal mol^{-1} $Å^{-2}$ at each round, with 50 ps MD simulation. Further, the system was slowly heated from 100 to 310 K over a period of 20 ps. The equilibration was continued over 50 ps after these 20 ps. A 3 ns simulation has been conducted for each enzyme/substrate complex.

Binding free energy

The MM-PBSA approach supplied with AMBER has been chosen because it is an efficient method to estimate free energy differences considering a series of ligands, or as here, to rank various binding mode of the same ligand. Such procedures have been tested previously and support this choice.[46] Using an interval of 1 ps, 3000 structures were extracted from each of our 3 ns of production runs. The electrostatic contribution to the solvation free energy was estimated using the modified Generalized Born (GB) model described by Onufriev *et al.*[47] To account for the influence of the solvent, an implicit solvent with a dielectric constant of $\varepsilon = 80$ has been applied. The salt concentration was fixed to zero. The nonpolar contribution to the solvation free energy due to cavity formation and van der Waals interactions between the solute and the solvent was estimated using the LCPO method.[48,49] The surface tension was set to 0.0072 kcal mol^{-1} $Å^{-2}$. Entropy contributions have been performed with the quasi-harmonic analysis in the ptraj module rather then using the normal mode analysis module implemented in MM-GBSA.

RESULTS AND DISCUSSION

Structural analysis

The three systems remain stable throughout the simulations as reflected by the low RMSd values (1.46, 1.62, and 1.80 Å for ES1, ES2, and ES3 respectively) computed using the starting structures as a reference. The residues showing the highest mobility (20–56) belong to the N-terminal domain, a small eight-stranded β-barrel composed of two antiparallel sheets known as a PLAT (Polycystin-1, Lipoxygenase, Alpha-Toxin) domain and found in a variety of membrane or lipid associated proteins.[50] These residues correspond to the loop connecting strands β1 and β2 and are close enough to the substrate cavity entrance so that their motion should influence the access to the active site. Throughout the various ES trajectories, the metal center (belonging to the C-terminal domain) remains tightly bound to its five initial residues, the sixth coordination being occupied by the substrate. With a $OD1_{Asn713}$-Fe distance of 3.81 Å in the high resolution native structure (i.e. 1RRH, and 3 Å in the medium resolution one 1LNH), Asn713 is weakly bound to the iron center. Solomon *et al.*[17] underlines the crucial role of the Asn694 ligand (which corresponds to Asn713 in LOX-3) in the catalytic mechanism of LOX-1. They have shown that the reduction of the ferric Fe(III) state to the catalytically inactive ferrous Fe(II) one generates a modification of the metal coordination. With the decrease of the Fe-$OD1_{Asn713}$ distance, the trigonal bipyramid structure of the active site is replaced by a distorted octahedral one. This is in good agreement with a higher Fe-$OD1_{Asn713}$ distance value in the case of an inhibitor like EGC (1JNQ) and lower ones in our E/S complexes than in the native structure.

Throughout the simulations, quercetin structure show deformations induced by the movements of the amino acids of the inner part of the cavity. Indeed, pyramidalization at the C2 carbon atom is reported for the three binding modes as reflected by the $\theta_{C2O1C3C1'}$ improper dihedral angle around the C2 carbon atom of quercetin that fluctuates between $-10°$ and $+10°$. Furthermore,

rotation around the C2 carbon atom is also reported for each binding mode. Average value of the O1C2C1′C2′ torsion angle is 35.9°, 33.8°, and roughly 20° for 3-OH, 7-OH, and 4′-OH binding modes, respectively. Such deformations are important since, as already presented in another dioxygenase (Q23D)/quercetin complex, they facilitate the dioxygen addition on quercetin.[31]

3-OH binding mode

Along the ES1 trajectory, O3 atom remains tightly bound to the iron center. The metal–ligand distance does not present significant fluctuations. A distorted octahedral geometry is observed around the active site throughout the simulation. Quercetin is stabilized in the pocket by two hydrogen bonds between 7-OH and O_{Thr274} and between 4′-OH and $OE1_{Gln514}$ (respective average distances 2.89 Å and 2.71 Å). The latter is also in interaction with a solvent molecule as shown in Figure 2. The 3′-OH functional group is also engaged in a stabilizing electrostatic interaction with oxygen atom (O) of residue Gln514 (average distance of 3.21 Å). Various hydrophobic interactions, mainly CH-π ones, involving Ala561, four leucine residues (277, 560, 565, 773) and the highly delocalized structure of quercetin increase the stabilization of the flavonoid substrate in the active site. Although quercetin is not the natural ligand of the LOX-3 enzyme, the substrate cavity adjoining the metal center is not only flexible enough to adapt the volume and shape of the substrate but also to leave solvent molecules filling in the extended part of the pocket, clearly separated from the main cavity.[21,23] In addition, the heterocycle of the flavonoid is positioned in the vicinity of the dioxygen cavity as already defined in various publications.[51,52]

7-OH binding mode

Three distinct periods are found along the ES2 dynamics depending on the Fe-substrate distance [see Fig. 3(a)]. In the starting structure, quercetin is quite distant from the active site. Fe—O7 distance is about 5 Å and decreases during the 400–900 ps period to an average value of 2.2 Å. Then, the Fe-O7 distance fluctuates during a 500 ps period (900–1400 ps) to finally reach an average value of 4 Å until the end of the simulation (1400–3000 ps). The position of the substrate is correlated to the C-terminal binding mode. During the first period (0–400 ps), O1 and O2 atoms of the C-terminal residue are both coordinated to the iron center ($d_{O1\text{-}Fe} \approx d_{O2\text{-}Fe} \approx 2.2$ Å). Then, Ile857 is connected to the metal in a monodentate way, via its O2 atom during the second period (400–1400 ps) and then via its O1 atom during the third one (1400–3000 ps).

In addition to strong electrostatic interaction with the metal center, quercetin interacts with amino acid of the inner part of the cavity through H-bonds involving

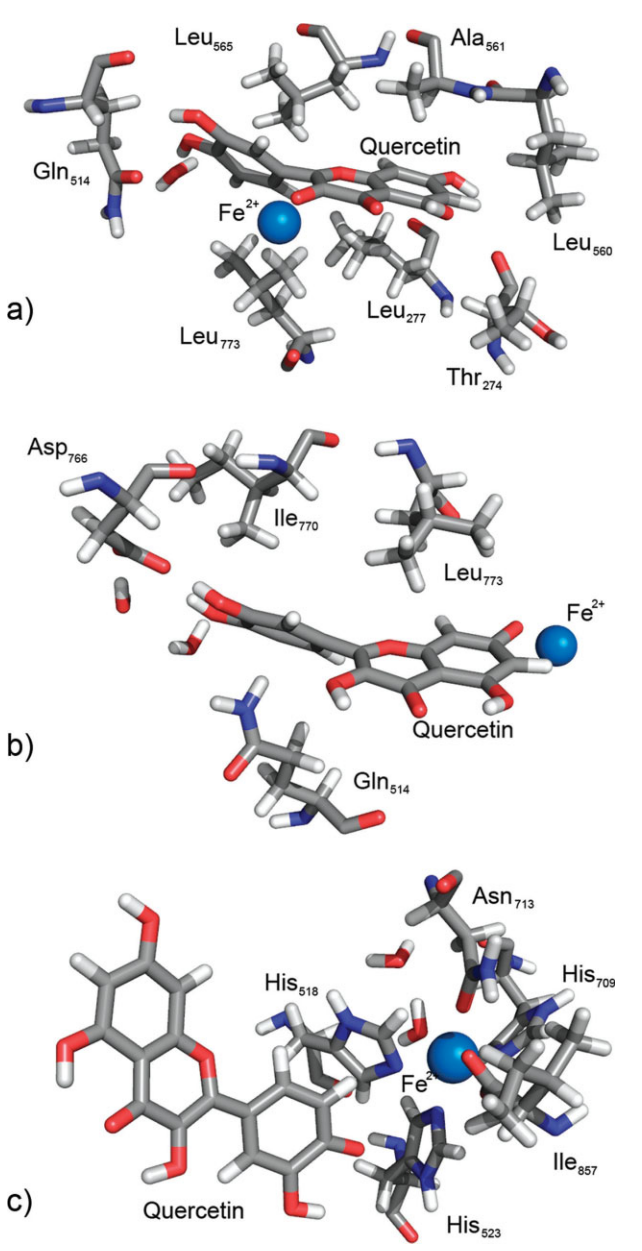

Figure 2

*Snapshots of the active site structures for **a**) ES1, **b**) ES2 and **c**) ES3 simulations.*

hydroxyl groups of the B-ring. 3′-OH hydroxyl group is directly linked with OD1 atom of the Asp766 sidechain, the average $O3'_{quercetin}$-$OD1_{Asp766}$ distance is 2.59 Å. In contrast, 4′-OH hydroxyl group is connected to $OD2_{Asp766}$ oxygen atom via a hydrogen bond network involving two water molecules [see Fig. 2(b)]. These solvent molecules, located in the extended part of the cavity, are closed to the entrance of the classical LOX-3 substrate. They present significant residence time over nanosecond range time scale. Although they could be

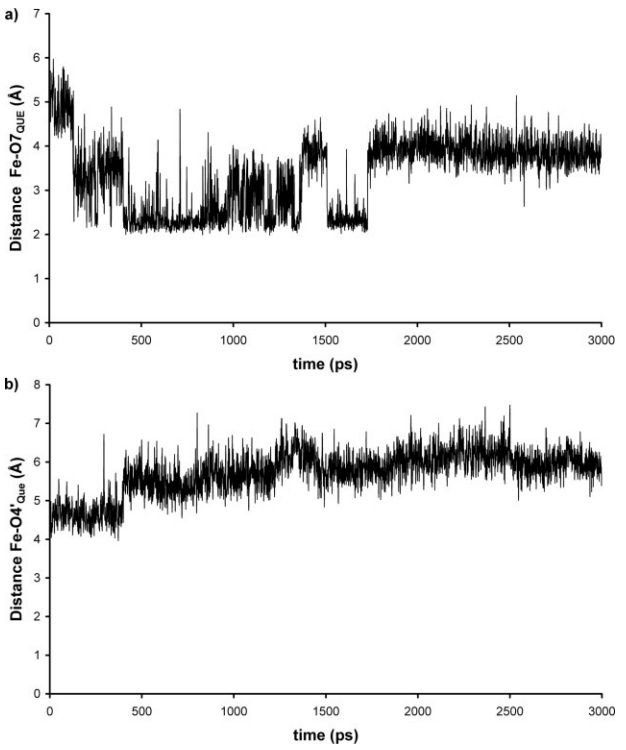

Figure 3

*Fluctuations of the Fe-quercetin distance throughout the trajectories: **a**) ES2 and **b**) ES3 simulations.*

exchanged with other solvent molecules, they play a structural role in the active site stabilizing the substrate in a nonplanar structure. Additionally, weak enzyme/substrate interactions involving Ile770, Leu773, and Gln514 residues also stabilize the substrate through many CH-π and NH-π interactions.

4′-OH binding mode

Although initially located in the first coordination sphere of the metal center, quercetin moves away from its first position during the thermalization/equilibration phase, to be quite distant from the metal center in the starting structure of the production run. Then Fe—O4′ distance fluctuates around 4.5 Å during the first 400 ps, whereas O1 and O2 atoms of the C-terminal residue both lie in the first coordination sphere of metal center. After 400 ps, the entrance of solvent molecules leads to an evolution of the coordination around the metal. They are initially located in a crevice partly covered by the six stranded barrel-like feature, the H6 and H7 helix, and the preceding coil (residues 349–488). As shown in Figure 3(b), after 410 ps, quercetin is pushed away of the active site during the iron-ligand swap, the Fe—O4′ distance increases and the substrate is then located at the entrance of the main cavity and in the extended part of it. In the meantime, a water molecule enters in the first coordination sphere and Ile857 is connected to the iron center in a monodentate way, alternatively via O2 or O1 oxygen atom. Figure 2(c) highlights the position of the water molecule in the opposite chelation site of the C-terminal residue. A pin-like loop (residue Pro384 to Thr402) presents the highest mobility of the region wrapping the crevice described above and one could imagine it governs the release of the substrate, opening an access to the metal center for solvent molecules. This, however, has to be analyzed with care because during this release iron center net atomic charge could change and standard pairwise additive potential cannot reproduce such effects.

Quercetin motion in the cavity is partly driven by the formation of a hydrogen bond network involving sidechain of residue Gln716 and Asp766, a water molecule and the 7-OH hydroxyl group of quercetin. It is surprising to note that Asp766-$O7_{quercetin}$ distance remains almost constant all along the simulation (average distance $O7_{quercetin}$-$OD1_{Asp766} \approx 2.62$ Å), in contrast with the decrease of the $HE2_{Gln716}$-$O7_{quercetin}$ distance (from $\sim$ 5 Å to 3 Å). This reinforces the idea that LOX-3 pocket is flexible enough to adapt to the shape and volume of the substrate.[23]

Binding free energy

To assess the predictive character of our approach, we have computed the binding free energy for each structure, based on an end-point approach, the so-called MM-GBSA model. The present calculation has the advantage of providing informations about the recognition of the ligand by the protein binding cavity from a quantitative point of view. The binding free energy, as well as its various components as predicted by MM-GBSA are compiled in Table I. The binding free energy includes the various components of the entropy term ($T\Delta S$), obtained by a quasi-harmonic analysis. The con-

Table I

Binding Free Energy Differences (in kcal/mol) for the Three Quercetin/LOX-3 Complexes and Contribution of Each Energetic Terms[a]

	ES1	ES2	ES3
ΔE_{ELE}	−78.6 (6.7)	−51.3 (7.0)	−27.7 (3.1)
ΔE_{VDW}	−36.4 (3.8)	−34.8 (3.7)	−39.7 (2.7)
ΔE_{GAS}	−115.0 (5.4)	−86.1 (5.6)	−67.4 (2.7)
ΔG_{SA}	−5.4 (0.1)	−5.7 (0.1)	−5.6 (0.1)
ΔG_{GB}	85.6 (4.4)	65.1 (5.1)	47.1 (1.8)
ΔG_{SOL}	80.2 (4.3)	59.5 (5.1)	41.5 (1.8)
$\Delta G_{GAS\ +\ SOL}$	−34.8 (3.2)	−26.6 (3.2)	−25.9 (2.5)
$T\Delta S$	−29.7	−30.1	−30.5
ΔG	−6.9	1.7	2.8

[a] E_{ELE}, coulombic energy; E_{VDW}, van der waals energy; G_{SA}, nonpolar term solvation free energy; G_{GB}, polar solvation free energy; TS, sum of the vibrational, rotational, and translational entropy term; $E_{GAS} = E_{ELE} + E_{VDW} + E_{INT}$; $G_{SOL} = G_{SA} + G_{GB}$; $G_{GAS+SOL} = H_{GAS} + G_{SOL}$; $G = G_{GAS+SOL} + H_{trans/rot} - TS$.

tribution $H_{trans/rot}$ due to the six translational and rotational degrees of freedom is equal to 3^*RT ($\approx$1.8 kcal mol^{-1}). This term is omitted in the MM-PBSA approach and should therefore be added to the total binding free energy. The different contributions of the free energy are obtained with quite low-standard deviation, revealing that the molecular dynamics trajectories sampled systems located in a conformational attractor, without large fluctuations at the ligand/receptor interface.

There is a striking difference between ES1 on one hand, where the binding free energy is negative (−6.9 kcal/mol), and ES2, ES3 on the other hand, where the calculations lead to positive binding free energies (1.7 and 2.8 kcal/mol). Clearly, only ES1 corresponds to a system representing a real affinity between the ligand and the receptor contrarily to ES2 and ES3.

The free energy differences are mainly driven by electrostatic terms (ΔE_{ELE} and ΔG_{GB}). The first one is connected to the coulomb interaction between the ligand and the receptor, independently of the surrounding solvent. Here, it is mainly originated by the interaction between the highly charged metal center and the substrate oxygen atoms (O3, O7, or O4′). ΔE_{ELE} ranking indeed follows the average substrate/metal distances (2.09, 3.35, and 5.71 Å for ES1, ES2, and ES3 respectively). The second term (ΔG_{GB}) estimates the coulomb contribution arising from the solvent and represents a major part of the so-called "desolvation penalty." This component has to be overcome during the binding event because it represents the electrostatic cost of withdrawing water molecules both within the binding pocket and around the solute, for the enzyme to accommodate the substrate. Note that the desolvation penalty is rather qualitatively consistent with the dipole moment of the quercetin substrate. It is larger for the substrate involved in ES1 (4.31 D, obtained at the B3LYP/6-31+G* level) than for those involved in ES2 or ES3 (3.61 and 3.81 D).

The entropic contribution is essentially due to the loss of mobility of the ligand when it binds the receptor. Our estimation of the $T\Delta S$ term is quite large, revealing a tight interaction between the substrate and the residues belonging to the protein cavity.

On the basis of both structural and energetic analyses, the so-called "3-OH" binding mode appears to be the most stabilizing in the case of an activation of the substrate via a deprotonation by the C-terminal residue, leading to an electron transfer to the metal center. Hence, this binding mode is the only one for which the binding free energy is negative revealing thus the most stable complex among the three possibilities. Although the three considered binding modes lead to similar structural modifications on the substrate (bending and pyramidalization), the 3-OH binding mode is the only one for which quercetin-Fe distance reflects a complexation during the simulation. This suggests that such an activation mode generate a stable enzyme/substrate intermediate prior degradation.

Different mechanisms can be envisaged that can lead to the degradation of the substrate. First, reaction with molecular dioxygen can be considered, and thus the way O2 enters the cavity has to be taken into account. Structurally speaking, in the ES1 simulation, the so-called dioxygen cavity points toward the substrate C2C3 double bond. This is not directly the case in ES2 and ES3. A direct addition of the dioxygen on the semiquinone species could then avoid the formation of the Enz-Fe-O-O-R intermediate and should explain why no "purple-state" of LOX was reported in the experimental study.[24] Such an addition of oxygen on quercetin has already been described in another work dedicated to the oxygenolysis of flavonoid.[41] In this work, all the structural requirements to accommodate a dioxygen molecule at the active site (a carboxylate functional group near the transition metal) and at the substrate (bending/pyramidalization) are present in this ES1 complex.

Other mechanisms could be considered to explain the quercetin degradation.[29,30] X-ray radiations could generate free radicals leading to the formation of highly quercetin reactive species (quinone and semiquinone) facilitating therefore the cooxidation process. Makris and Rossiter[30] suggest in their work, a hydroxyl free-radical-mediated oxidation in the presence of a copper(II) cation. The mechanism requires the chelation of one of the possible binding sites to a transition metal. A recent study[53] enlightens the structural features required to inhibit 5-LOX, and the conclusions are in contradiction with a part of the proposed mechanism. Authors demonstrate that a substitution on the 3-hydroxychromone functional group of quercetin (quercetin-3-O-glucoronide and 3′-O-methylquercetin-3-O-glucoronide) preserves the LOX inhibitory activity, whereas it is not the case on the catechol moiety (quercetin-3′-O-sulfate and 3′-O-methylquercetin). One could imagine that sterical hindrance involving the B-ring could therefore prevent a stabilizing metal chelation. Moreover, we have previously shown that the chelation of a transition metal on the 5-hydroxychromone functional group leads to an electronic spin density mainly delocalized on the A-ring.[32] In such a way, ROS would not be added on the C-ring but on the C8 or C6 atom. In addition, taxifolin has no antiinflammatory activity[53] (inhibition of LTB_4 production), and its only structural difference with quercetin is the absence of the C2C3 double bond. Such conclusions confirm the important role of the 3-hydroxychromone functional group and support the addition of an oxidizing agent on the C2C3 double bond of the flavonoid. As a first phase of the multistep inhibition process, the quercetin oxygenolysis catalyzed by LOX-3, which we proposed is therefore conceivable.

CONCLUSIONS

Inhibition of LOX-3 enzyme by quercetin is effective but X-ray determination of the quercetin/LOX-3 complex

has not led to a clear depiction of the substrate/enzyme mode of binding. Furthermore, the fact that only a degradation product of quercetin has been found in the X-ray structure has led to a doubt concerning the exact role of the flavonol molecule in the inhibition of the enzyme. Acting both as a substrate and a source of inhibition, quercetin seems to play an antinomic role. But this could be explained as quercetin, one of the most representative flavonoids, is a highly functionalized substrate and can thus be activated and degraded following several ways. In this study, we have investigated three modes of enzyme/substrate interaction that are compatible with both hypotheses: a degradation process induced by the X-ray radiation protocol and catalyzed by the enzyme. Among the three considered modes of binding, it appears that quercetin should be linked to the metal center via its 3-OH functional group. The most favorable term to the binding free energy is due to electrostatic interactions. The entropic contribution of the binding free energy reveals that quercetin looses its flexibility and is strongly trapped inside the cavity. Moreover, residues constituting the active site impose structural modifications on the substrate that activate the C2 position (pyramidalization of the improper dihedral around C2 atom and bending of the O1C2C1′C2′ dihedral), awaiting a putative dioxygen addition that could lead to the degradation product. These results are in good agreement with experimental data that do not reveal the existence of the "purple state" of LOX which is a classical intermediate in PUFA degradation.

ACKNOWLEDGMENTS

CMIM (Centre de Modélisation et d'Imagerie Moléculaire) of the University of Nice and CINES (Centre Informatique National de l'Enseignement Supérieur) are greatly acknowledged for provision of computation time. Referee for this publication is greatly acknowledged for interesting and constructive remarks.

REFERENCES

1. Prigge ST, Boyington JC, Faig M, Doctor KS, Gaffney BJ, Amzel LM. Structure and mechanism of lipoxygenases. Biochimie 1997;79:629–636.
2. Coffa G, Schneider C, Brash AR. A comprehensive model of positional and stereo control in lipoxygenases. Biochem Biophys Res Commun 2005;338:87–92.
3. Kuhn H, Saam J, Sebastian E, Holzhütter H-G, Ivanov I, Walther M. Structural biology of mammalian lipoxygenase: enzymatic consequences of targeted alterations of the protein structure. Biochem Biophys Res Commun 2005;338:93–101.
4. Skrzypczak-Jankun E, Chorostowska-Wynimko J, Shelman SH, Jankun J. Lipoxygenases—a challenging problem in enzyme inhibition and drug development. Curr Enzyme Inhib 2007;3:119–132.
5. Jampilek J, Dolezal M, Opletalova V, Hartl J. Lipoxygenase. Leukotrienes biosynthesis and potential antileukotrienic agents. Curr Med Chem 2006;13:117–129.
6. Hu J, Huang Y, Xiong M, Luo S, Chen Y, Li Y. The effects of natural flavonoids on lipoxygenase-mediated oxidation of compounds with a benzene ring structure—a new possible mechanism of flavonoid anti-chemical carcinogenesis and other toxicities. Int J Toxicol 2006;25:295–301.
7. Kemal C, Louis-Flamberg P, Krupinski-Olsen R, Shorter AL. Reductive inactivation of soybean lipoxygenase 1 by catechols: a possible mechanism for regulation of lipoxygenase activity. Biochemistry 1987;26:7064–7062.
8. Withman S, Gezginci M, Timmermann BN, Holman TR. Structure-activity relationship studies of nordihydroguaiaretic acid inhibitors toward soybean, 12-human, and 15-human Lipoxygenase. J Med Chem 2002;45:2659–2661.
9. Galpin JR, Tiellens LGM, Veldink GA, Vliegenthart JFG, Boldingh J. On the interaction of some catechol derivatives with the iron atom of soybean lipoxygenase. FEBS Lett 1976;69:179–182.
10. Di Carlo G, Mascolo N, Izzo AA, Capasso F. Flavonoids: old and new aspects of a class of natural therapeutic drugs. Life Sci 1999;65:337–353.
11. Peterson J, Dwyer J. Flavonoids: dietary occurrence and biochemical activity. Nutr Res 1998;18:1995–2018.
12. Chi YS, Jong HG, Son KH, Chang HW, Kang SS, Kim HP. Effects of naturally occurring prenylated flavonoids on enzymes metabolizing arachidonic acid: cyclooxygenases and lipoxygenases. Biochem Pharmacol 2001;62:1185–1191.
13. Sadik CD, Sies H, Schewe T. Inhibition of 15-lipoxygenases by flavonoids: structure-activity relations and mode of action. Biochem Pharmacol 2003;65:773–781.
14. Minor W, Steczko J, Stec B, Otwinowski Z, Bolin JT, Walter R, Axelrod B. Crystal structure of soybean lipoxygenase L-1 at 1.4 ANG. resolution. Biochemistry 1996;35:10687–10701.
15. Coffa G, Imber AN, Maguire BC, Laxmikanthan G, Schneider C, Gaffney BJ, Brash AR. On the relationships of substrate orientation. Hydrogen abstraction, and product stereochemistry in single and double dioxygenations by soybean lipoxygenase-1 and its Ala542Gly mutant. J Biol Chem 2005;280:38756–38766.
16. Abu-Omar MM, Loaiza A, Hontzeas N. Reaction mechanisms of mononuclear non-heme iron oxygenases. Chem Rev 2005;105:2227–2252.
17. Solomon EI, Zhou J, Neese F, Pavel EG. New insights from spectroscopy into the structure/function relationships of lipoxygenases. Chem Biol 1997;4:795–808.
18. Nelson MJ, Seitz SP, Cowling RA. Enzyme-bound pentadienyl and peroxyl radicals in purple lipoxygenase. Biochemistry 1990;29:6897–6903.
19. Nelson MJ, Cowling RA. Observation of a peroxyl radical in samples of "purple" lipoxygenase. J Am Chem Soc 1990;112:2820–2821.
20. Skrzypczak-Jankun E, Bross RA, Carroll RT, Dunham WR, Funk MO, Jr. Three-dimensional structure of a purple lipoxygenase. J Am Chem Soc 2001;123:10814–10820.
21. Skrzypczak-Jankun E, Amzel LM, Kroa BA, Funk MO, Jr. Structure of soybean lipoxygenase L3 and a comparison with its L1 isoenzyme. Proteins: Struct Funct Genet 1997;29:15–31.
22. Skrzypczak-Jankun E, Borbulevych OY, Jankun J. Soybean lipoxygenase-3 in complex with 4-nitrocatechol. Acta Cryst 2004;D60:613–615.
23. Skrzypczak-Jankun E, Borbulevych OY, Zavodszky MI, Baranski MR, Padmanabhan K, Petricek V, Jankun J. Effect of crystal freezing and small-molecule binding on internal cavity size in a large protein: X-ray and docking studies of lipoxygenase at ambient and low temperature at 2.0 Å resolution. Acta Cryst 2006;D62:766–775.
24. Borbulevych OY, Jankun J, Selman SH, Skrzypczak-Jankun E. Lipoxygenase interactions with natural flavonoid, quercetin, reveal a complex with protocatechuic acid in its X-ray structure at 2.1 A resolution. Proteins: Struct Funct Bioinf 2004;54:13–19.
25. Skrzypczak-Jankun E, Zhou K, McCabe NP, Selman SH, Jankun J. Structure of curcumin in complex with lipoxygenase and its significance in cancer. Int J Mol Med 2003;12:17–24.

26. Skrzypczak-Jankun E, Zhou K, Jankun J. Inhibition of lipoxygenase by (−)-epigallocatechin gallate: X-ray analysis at 2.1A reveals degradation of EGCG and shows soybean LOX-3 complex with EGC instead. Int J Mol Med 2003;12:415–422.
27. van Acker SABE, van den Berg D-J, Tromp MNJL, Griffioen DH, van Bennekom WP, van der Vijgh WJF, Bast A. Structural aspects of antioxidant activity of flavonoids. Free Radical Biol Med 1996;20: 331–342.
28. Jungbluth G, Ruhling I, Ternes W. Oxidation of flavonols with Cu(II). Fe(II), Fe(III) in an aqueous media. J Chem Soc Perkin Trans 2 2000;9:1946–1952.
29. Krishnamachari V, Levine LH, Paré PW. Flavonoid oxidation by the radical generator AIBN: a unified mechanism for quercetin radical scavenging. J Agric Food Chem 2002;50:4357–4363.
30. Makris DP, Rossiter JT. Hydroxyl free radical-mediated oxidated degradation of quercetin and morin: a preliminary investigation. J Food Compos Anal 2002;15:103–113.
31. Fiorucci S, Golebiowski J, Cabrol-Bass D, Antonczak S. Molecular simulations bring new insights into flavonoid/quercetinase interaction modes. Proteins: Struct Funct Bioinf 2007;67:927–970.
32. Fiorucci S, Golebiowski J, Cabrol-Bass D, Antonczak S. DFT study of quercetin activated forms involved in antiradical. antioxidant, and prooxidant biological processes J Agric Food Chem 2007;55: 903–911.
33. Becke AD. Density-functional exchange-energy approximation with correct asymptotic behavior. Phys Rev A: At Mol Opt Phys 1988;38: 3098–3100.
34. Becke AD. Density-functional thermochemistry. III. The role of exact exchange. J Chem Phys 1993;98:5648–5642.
35. Lee C, Yang W, Parr RG. Development of the Colle-Salvetti correlation-energy formula into a functional of the electron density. Phys Rev B: Condens Matter Mater Phys 1988;37:785–789.
36. Ditchfield R, Hehre WJ, Pople JA. Self-consistent molecular-orbital methods. IX. An extended Gaussian-type basis for molecular-orbital studies of organic molecules. J Chem Phys 1971;54:724–728.
37. Hariharan PC, Pople JA. The influence of polarization functions on molecular orbital hydrogenation energies. Theor Chimica Acta 1973;28:213–222.
38. Clark T, Chandrasekhar J, Schleyer PvR. Efficient diffuse function-augmented basis set for anion calculations. III. The 3–21+G basis set for first-row elements, Li-F. J Comput Chem 1983;4:294–301.
39. Krishnan R, Binkley JS, Seeger R, Pople JA. Self-consistent molecular orbital methods. XX. A basis set for correlated wave functions. J Chem Phys 1980;72:650–654.
40. Frisch MJ, Trucks GW, Schlegel HB, Scuseria GE, Robb MA, Cheeseman JR, Zakrzewski VG, Montgomery JAJ, Stratmann RE, Burant JC, Dapprich S, Millam JM, Daniels AD, Kudin KN, Strain MC, Farkas O, Tomasi J, Barone V, Cossi M, Cammi R, Mennucci B, Pomelli C, Adamo C, Clifford S, Ochterski J, Petersson GA, Ayala PY, Cui Q, Morokuma K, Malick DK, Rabuck AD, Raghavachari K, Foresman JB, Cioslowski J, Ortiz JV, Baboul AG, Stefanov BB, Liu G, Liashenko A, Piskorz P, Komaromi I, Gomperts R, Martin RL, Fox DJ, Keith T, Al-Laham MA, Peng CY, Nanayakkara A, Gonzalez C, Challacombe M, Gill PMW, Johnson B, Chen W, Wong MW, Andres JL, Gonzalez C, Head-Gordon M, Replogle ES, Pople JA. Gaussian03, Revision C. 02. Wallingford, CT: Gaussian; 2003.
41. Fiorucci S, Golebiowski J, Cabrol-Bass D, Antonczak S. Oxygenolysis of flavonoid compounds: DFT description of the mechanism for quercetin. Chem Phys Chem 2004;5:1726–1733.
42. Wang J, Wang W, Kollman PA, Case DA. Automatic atom type and bond type perception in molecular mechanical calculations. J Mol Gr Modell 2006;25:247–260.
43. Pearlman DA, Case DA, Caldwell JW, Ross WS, Cheatham TE, III, DeBolt S, Ferguson D, Seibel G, Kollman P. AMBER, a package of computer programs for applying molecular mechanics, normal mode analysis, molecular dynamics and free energy calculations to stimulate the structural and energetic properties of molecules. Comput Phys Commun 1995;91:1–42.
44. Li J, Zhu T, Cramer CJ, Thuhlar DG. New class IV charge model for extracting accurate partial charges from wave functions. J Phys Chem A 1998;102:1821–1831.
45. Wang J, Wolf RM, Caldwell JW, Kollman PA, Case DA. Development and testing of a general AMBER force field. J Comput Chem 2004;25:1157–1174.
46. Charlier L, Nespoulous C, Fiorucci S, Antonczak S, Golebiowski J. Binding free energy prediction in strongly hydrophobic biomolecular systems. Phys Chem Chem Phys 2007;9:5761–5771.
47. Onufriev A, Bashford D, Case DA. Exploring protein native states and large-scale conformational changes with a modified generalized born model. Proteins: Struct Funct Bioinf 2004;55:383–394.
48. Weiser J, Shenkin PS, Still WC. Approximate Atomic Surfaces from linear combinations of pairwise overlaps (LCPO). J Comput Chem 1999;20:217–230.
49. Weiser J, Shenkin PS, Still WC. Fast approximate algorithm for detection of solvent inacessible atoms. J Comput Chem 1999;20: 586–596.
50. Bateman A, Sandford R. The PLAT domain: a new piece in the PKD1 puzzle. Curr Biol 1999;9:R588–R590.
51. Youn B, Sellhorn GE, Mirchel RJ, Gaffney BJ, Grimes HD, Kang C. Crystal structures of vegetative soybean lipoxygenase VLX-B and VLX-D, and comparisons with seed isoforms LOX-1 and LOX-3. Proteins: Struct Funct Bioinf 2006;65:1008–1020.
52. Saam J, Ivanoc I, Walther M, Holzhütter H-G, Kuhn H. Molecular dioxygen enters the active site of 12/15-lipoxygenase via dynamic oxygen access channels. Proc Natl Acad Sci USA 2007;104:13319–13324.
53. Loke WM, Proudfoot JM, Stewart S, McKinley AJ, Needs PW, Kroon PA, Hodgson JM, Croft KD. Metabolic transformation has a profound effect on anti-inflammatory activity of flavonoids such as quercetin: lack of association between antioxidant and lipoxygenase inhibitory activity. Biochem Pharmacol 2008;75:1045–1053.